Chemical Geology 387 (2014) 144–156

Contents lists available at ScienceDirect

Chemical Geology

journal homepage: www.elsevier.com/locate/chemgeo

The Archean magmatic-hydrothermal system of Lac Shortt (Au-REE), Abitibi, Canada: Insights from carbonate fingerprinting

Olivier Nadeau [a,b,*], Ross Stevenson [a,b], Michel Jébrak [a]

[a] Université du Québec à Montréal, Montréal, Canada
[b] Geotop Research Centre in Geochemistry and Geodynamics, Montreal, Canada

ARTICLE INFO

Article history:
Received 3 March 2014
Received in revised form 15 August 2014
Accepted 19 August 2014
Available online 29 August 2014

Editor: K. Mezger

Keywords:
Gold and REE deposits
Mantle magmatism-hydrothermalism
Carbonatites
Syenites
Lamprophyres
Carbonate fingerprinting

ABSTRACT

Trace element and isotopic data from the Lac Shortt (Abitibi, Canada) gold and rare earth element (REE) deposit sheds light on the cogenetic association between alkali magmatism (syenites and lamprophyres), carbonatation (magmatic and carbothermal) and gold – REE mineralization. Magmatic and carbothermal carbonates from comagmatic lithologies from the Lac Shortt gold-REE deposit were analyzed for major, minor and trace elements concentrations as well as for their $^{87}Sr/^{86}Sr_0$, $\delta^{13}C$ and $\delta^{18}O$ isotopic ratios. Carbonates from Lac Shortt have $\delta^{13}C$ values ranging from −4.89 to 2.38 ‰ VPDB and $\delta^{18}O$ values ranging from 8.28 to 15.02. The lightest values are found in carbonate from the carbonatites and the heaviest values are associated with the ore-carbonates. Carbonates from the various lithologies lie between these two extremes. Initial $^{87}Sr/^{86}Sr$ ratios from the carbonates cluster tightly around 0.7013–0.7016, i.e., depleted Archean mantle signatures, although some have slightly more radiogenic values, from 0.7026 to 0.7029. The small variation in the strontium isotope ratios compared to the C and O isotopic values suggests that carbonate anions (CO_3^{2-}) were decoupled from the cations during hydrothermal alteration. Cations such as Sr^{2+} and Ca^{2+} in carbonates from the high grade ore and from magmatic and hydro-carbothermal carbonatite appear to originate from the Late-Archean, depleted mantle. Since gold is a cation and is strongly associated with carbonatite magmatism and associated carbo-hydrothermal carbonatation, we suggest gold too has a depleted mantle origin. The carbonates are enriched in mobile high field strength elements (HFS; Ba, Sr) elements, depleted in immobile HFS elements (Th, U, Ta, Nb, Zr, Ti) and have enriched- to slightly depleted REE patterns with flat to strong light-REE enrichments. These trace element concentrations support the fact that all the lithologies were comagmatic and that the ore itself was genetically related to these lithologies. Based on present day knowledge of Archean tectonics of Abitibi, post collision extension tectonics and mantle delamination, isotope geochronology, on the magmatic-hydrothermal system of Lac Shortt itself and on the present paper's carbonate fingerprinting, we propose that Lac Shortt calc-alkaline dioritic magmatism-hydrothermalism was followed by alkaline syenitic, and eventually carbonatitic magmatism-hydro-carbothermalism, and that gold and REE originated from the carbonatite magmatic-carbo-hydrothermal system and its mantle roots, which agrees with mass balance calculations. The depleted-mantle-rooted, carbonatite exsolved a hydro-carbothermal fluid enriched in REE and gold which fenitized and oxidized the syenite and out of which the gold and REE mineralization was deposited.

1. Introduction

Following Groves et al.'s (1998) classification of 'orogenic' gold deposits, Robert (2001) demonstrated that not all 'orogenic' gold deposits originate from orogeny and that there is at least one distinct class of non-orogenic magmatic-hydrothermal gold deposits in the Abitibi Archean greenstone belt. The magmatic-hydrothermal gold deposits of the Abitibi display disseminated as well as vein-hosted gold-sulfide mineralization, potassic (K feldspar, biotite or sericite) and carbonate alteration, and are associated with syenitic to monzonitic rocks and dikes. These deposits are often found in close association with post-orogenic Timiskaming-type conglomerates and are of Timiskaming age (2680–2672 Ma). The genesis of this class of deposit remains obscure and the present paper aimed at deciphering the origin of such mineralization by studying the Lac Shortt deposit, near Lebel-sur-Quévillon (Morasse, 1988; Prud'homme, 1990; See, 1994; Tilton and Bell, 1994; Brisson, 1998; Nadeau et al., 2012).

The Lac Shortt Au-REE deposit hosted 2.7 Mt of ore at an average of 4.6 g/t Au (total 12.4 tons Au; Brisson, 1998). The mineralization was associated with a complex suite of intrusions consisting of alkali gabbros, syenite, carbonatite and silicocarbonatite plugs and dykes, undifferentiated mafic and dioritic sills, and ultramafic, calc-alkaline and alkaline lamprophyres (Morasse, 1988; Prud'homme, 1990; Bourne and Bosse,

* Corresponding author.
E-mail address: onadeau@uottawa.ca (O. Nadeau).

http://dx.doi.org/10.1016/j.chemgeo.2014.08.021
0009-2541/

1991; See, 1994). The Lac Shortt deposit is both locally (Prud'homme, 1990) and regionally (Dolodau carbonatite; Bedard, 1988; Bedard and Chown, 1992) associated with coeval carbonatite magmatism. The syenite-lamprophyre-carbonatite-gold association at Lac Shortt provides a unique opportunity to study the role of the carbon-rich fluids associated with magmatic hydrothermal gold deposits of the Abitibi.

This paper presents new geochemical and isotopic ($\delta^{13}C$, $\delta^{18}O$ and $^{87}Sr/^{86}Sr$) data from carbonate minerals of the Lac Shortt carbonatite-lamprophyre-syenite-gold ore system that constrain both the petrogenesis of the magmatic system as well as the metallogenesis of the associated gold-REE deposit. At Lac Shortt, both magmatic and carbo-hydrothermal carbonates are present in carbonatites, silicocarbonatites, hornblendites, lamprophyres, mafic and dioritic sills, syenites and high and low grade ores. The geochemical and isotopic fingerprinting of carbonates from carbonatites, silicocarbonatites, mafic and dioritic sills, syenites and ores confirm that they have a common origin (Prud'homme, 1990) and sheds light on the ore-generating processes. Furthermore, the use of Sr isotopes as a proxy for solutes and C and O isotopes as proxies for solvents suggest that solutes present in these carbonates originated from the Late-Archean, sub-continental depleted mantle and that the solvents within the same crystals gradually equilibrated with the Archean crust during hydro-carbothermal alteration. Finally, as mineralization is intimately associated with carbonatization at Lac Shortt (Prud'homme, 1990; See, 1994; Brisson, 1998), the comparison of carbonates from Au ore and other lithologies suggest that gold was transported and deposited by mantle-derived, aqueous-carbonic fluids that exsolved from the carbonatite at emplacement depths and deeper.

2. Geological context

The Lac Shortt alkaline complex is located in the eastern Abitibi greenstone belt and is hosted by tholeiitic volcanic flows of the Wachigabau Formation and sediments of the Dalime formation (Brisson, 1998).The Lac Shortt deposit (Fig. 1) is embedded in ENE Lac Shortt fault, which is a secondary splay of the major Lamarck NE-SW shear zone (Brisson, 1998). Intrusions of the Lac Shortt alkaline complex were emplaced syn- to late-deformation within- and channelized by this shear zone. The alkaline complex contains the oldest carbonatite in Canada (2652 Ma; Morasse, 1988), undifferentiated mafic sills, massive and dike-like syenites and carbonatites, hornblendite dikes, diorite sills, calc-alkaline, alkaline and ultramafic lamprophyres (Bourne and Bosse, 1991) dikes and carbo-hydrothermal gold mineralization. The Lac Shortt fault zone contains blocs and clasts of carbonatites and syenites and the carbonatite contains syenite boudins.

2.1. Syenites

Fresh syenite contains K feldspar, albite, biotite, muscovite, dolomite, calcite, pyrite, magnetite, hematite, apatite and monazite (Morasse, 1988). Quartz, calcite and fluorite are present in veinlets. The altered syenite is mylonitized, oxidized to brick-red and contains ankerite, more abundant K feldspar and hematite, and is enriched in Au, Ba, Sr, Ca and CO_2 compared to the fresh syenite. The syenite dikes also contain sphalerite, galena, pyrrhotite, rutile and leucoxene, fluorite, barite, pyrochlore, cerianite ($[Ce^{4+},Th]O_2$), bastnaesite ($[Ce,La]CO_3F$), zircon, aikinite ($PbCuBiS_3$) (Morasse, 1988). The syenite has abnormally high levels of K_2O (up to 12 wt.%) and low levels of Na_2O (<1 wt.%), caused by metasomatism (Morasse, 1988). Zoned microcline is interpreted to result from potassic metasomatism. Calcite is observed in the syenite dikes as sheet-like structures interpreted to originate from the carbonatite. This is in agreement with the presence of pyrochlore, bastnaesite and monazite both in the carbonatite and the syenite and is corroborated by the existence of a hybrid carbonatite-syenite dike, having a core of red syenite injected and fragmented by calcite, an external envelope of carbonatite which appears to intrude the syenite, and a reaction texture at the contact between both units. This dike is interpreted to result from the intrusion of a syenite and subsequently by the injection of the carbonatite (Morasse, 1988). The

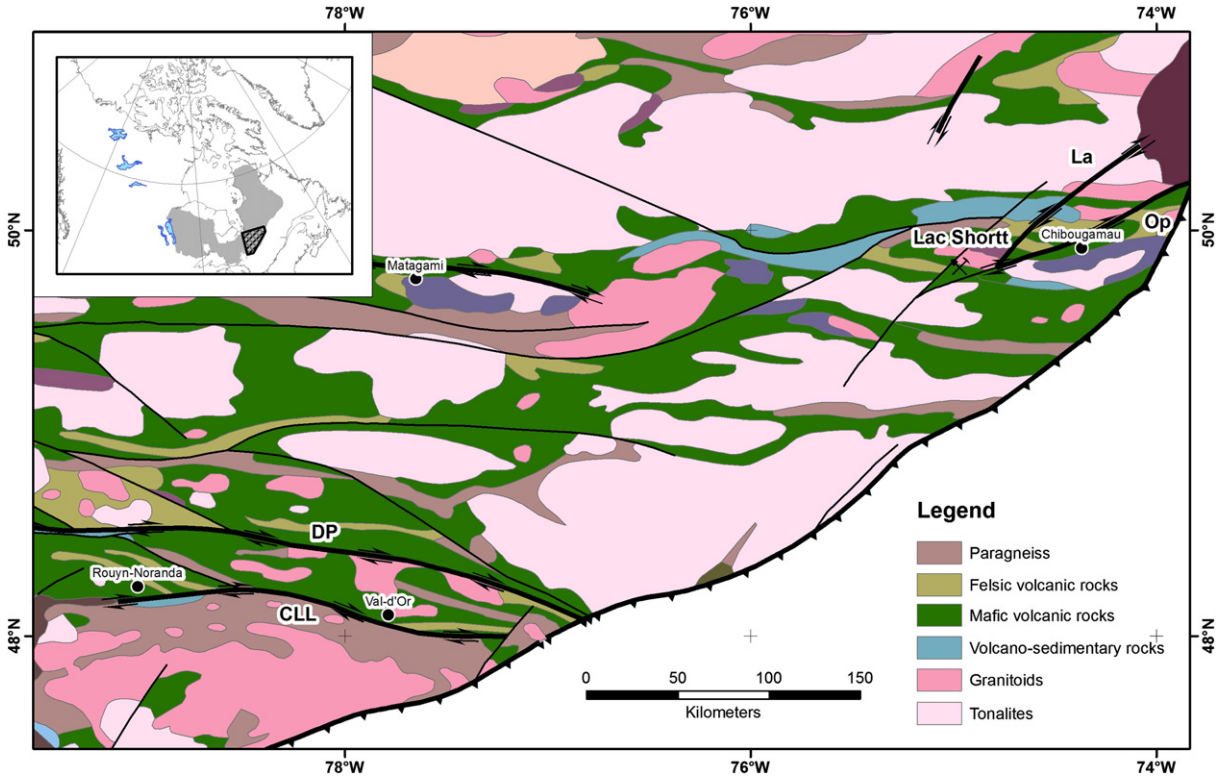

Fig. 1. Geological map of Abitibi. Lac Shortt is located in northeastern Abitibi, near the intersection of the Lamarck (La) and the Opawica (Op) regional faults. Rouyn and Val d'Or are shown between the Cadillac – Larder Lake (CLL) and the Destor Porcupine (DP) fault zones for reference. Southeastern Abitibi is in structural contact with the Province of Grenville (in white). The inset shows the localization of the map in the Archean Province of the Superior (in gray) and in North America.

presence of shreds of syenite in the carbonatite makes it post-syenitic and the presence of sheared and deformed dikes of carbonatite in the ore makes it early- to syn-tectonic. Lead isotopes on galena in syenite returned a model age of 2665–2680 Ma while Pb in galena in carbonatite was dated at 2652 Ma (error not reported; Thorpe et al., 1984; Morasse, 1988). Potassic and sodic fenitization episodes at Lac Shortt may be associated to magmatic-hydrothermal activity of the syenite and the carbonatite, respectively (Prud'homme, 1990).

2.2. Carbonatites

The carbonatite is a sövite with > 90% calcite containing multiple shreds of syenites (Prud'homme, 1990). It takes the form of a massive intrusion as well as numerous dikes. It contains biotite, apatite, feldspars, magnetite and pyrite (Prud'homme, 1990). Part of the biotite is metasomatic (Wilhelmy and Kieller, 1986). The carbonatite is sometimes mylonitized and can also be present as the matrix of a breccia with clasts made of silicate rock. The carbonatite is enriched in light REE (LREE), Ag (6 ppm), Ba, Th, U, Pb, Sr and Zr as reflected in the presence of zircon, pyrochlore, ancylite (Sr and LREE hydrated carbonate) and synchysite (Ca and LREE fluorocarbonate), bastnaesite (LREE fluorocarbonate), as well as fluorite, magnocolumbite, aegirine, riebeckite, chalcopyrite, pyrrhotite, hematite, monazite, barite, celestite. It is relatively depleted in Rb, K, Hf, Ti and HREE (Morasse, 1988). Carbonatite and syenite are interpreted to be comagmatic (Tilton and Bell, 1994) and appear to have evolved under relatively oxidizing conditions while breccias and gold veins returned fO_2 estimates with values below the QFM buffer (See, 1994).

2.3. Lamprophyres

The alkali lamprophyre (a monchiquite) dike is about 10 cm wide, panidiomorphic, partly serpentinized, contains phenocrysts of olivine and phlogopite in a carbonatized-, magnetite and ilmenite-rich groundmass (Morasse, 1988). It contains ultramafic xenoliths with olivine rimmed by serpentine partly replaced by talc, magnetite, calcite and quartz. The hornblendite, possibly a calc-alkaline lamprophyre (vogesite, with K feldsdpar > plagioclase, to spessartite, with plagioclase > K feldspar) consists of euhedral hornblende with apatite and olivine in a groundmass of secondary calcite, chlorite and epidote. Ultramafic and calc-alkaline lamprophyres trace element geochemistry collected mainly from drill cores in a radius of 10 km around Lac Shortt mine have ubiquitous phogopite, olivine replaced by serpentine-chlorite-magnetite-carbonates, apatite, perovskite and ilmenite (Bourne and Bosse, 1991). Calcite is abundant in the matrix replacing olivine or as veinlets. Strontium, Th, Ce, P, Zr, Hf, Sm and Yb were immobile while LILE (Ba, Cs, Rb, K) were mobile during alteration (Bourne and Bosse, 1991; Wyman and Kerrich, 1989). The lamprophyres have negative Ta, Nb and Ti anomalies.

2.4. Fluid inclusions

Fluid inclusions were identified with temperatures of homogenization varying mainly between 190 and 350 °C, reaching up to 510 °C in carbonatite, and pressures mainly between 130 and 320 MPa, reaching up to 450 MPa in gold-quartz veins, and as low as 180–220 MPa during brecciating events (See, 1994). Numerous inclusions display boiling (co-existing liquid- and vapor-rich fluid inclusions) assemblages. Homogenization of fluid and melt inclusions in carbonatite occurred at less than 600 °C and around 900–950°C in syenite. Fluid temperature estimates from oxygen isotope data agree with those obtained from fluid inclusion homogenization temperatures (See, 1994).

2.5. Mineralization

The mineralization at Lac Shortt is distinct from other gold deposits of the area by: (1) Its disseminated texture; (2) no, or accessory-only quartz veins; (3) red hematization; (4) metasomatic potassic feldspar and (5) small, felsic and alkaline intrusions (Brisson, 1998). The carbonatite and the gold mineralization are contemporaneous (Prud'homme, 1990). The ore is divided into 3 types: the high grade, the low grade and the carbonatite ores. The high grade ore is enriched in pyrite and has 10–12 g/t Au; the low grade ore is enriched in hematite and hosts 3–6 g/t Au; the carbonatite ore has 1–3 g/t Au (Morasse, 1988; Brisson, 1998). The ore is described as a pyrite-rich mylonite with fragments of the embedding syenite. The protolith is thought to have been an alkali gabbro (not sampled in the present study) based on a transition at depth, where the gold stops being hosted by the mylonite and is instead hosted by this gabbro (Brisson, 1998). The gold is closely associated with pyrite and often found in tiny fractures within pyrite grains (See, 1994) as in many other gold syenites in the Abitibi (e.g., Bigot, 2012). Gold within pyrite or in the matrix of the mylonite is present as particles about 6 microns in diameter.

3. Methodology

3.1. Major element compositions

Carbonates were analyzed using a JEOL JXA-8900L electron microprobe (EMP) with a twenty to forty micron defocused beam, 15 kV and 20 nA in the Geochemical Laboratories at McGill University, Montreal, Canada. The instrument was calibrated using a set of Cameca and Canmet mineral standards and in-house calcite and dolomite standards. Relative errors (1σ) are generally less than 1% (e.g., CaO = 50 ± 0.5 wt.%). Counting times were 20 s for all elements except for Ba and Rb. Barium was initially analyzed for 60 s but was always below the limit of detection (LOD) of 600–650 ppm. Trials at 120 s return Ba below the LOD of 400–460 ppm so Ba was not analyzed using the electron probe. Similarly, Rb was first tried using a counting time of 120 s but turned out to be below the LOD of about 400–450 ppm. Subsequent trials at 200 s returned Rb values below the LOD of about 100–150 so it was not analyzed using the electron probe.

3.2. Strontium isotope data

Carbonates were extracted using a microdrill equipped with a 100 μm diameter diamond drill bit or using a simple drill equipped with a small diamond drill bit. A fraction of this powder was set aside for stable isotope analyses (see the following section). The powdered samples were soaked twice in 0.2 M ammonium acetate for 30 min in order to remove loosely bound Sr cations produced by the decay of Rb. Samples were then dissolved in 0.5 M acetic acid on hot plates for 2 h, subsequently centrifuged, and the supernate was pipetted out and dried overnight. Dry samples were dissolved in 3N HNO_3 and eluted twice through teflon columns with Sr-specific resin. These procedures were performed in a class 100 (ISO5) clean room at Geotop, UQAM. The Sr samples were loaded on Re filaments and analyzed using a Thermo Scientific Triton Plus thermal ionization, magnetic sector mass spectrometer (TIMS) at the Geotop. A NBS987 standard was used before and after each run returning $^{87}Sr/^{86}Sr$ value of 0.70125 ± 0.00001 2σ standard error. For each sample the Rb signal was initially low and was subsequently burnt off before initializing the analytical procedure.

3.3. Carbon and oxygen isotope data

A polished section of each sample was first analyzed by electron microprobe to identify the types of carbonates. For calcites about 120 μg, and for other carbonates about 150–450 μg of sample was weighed into a glass micro-crucible using a micro-balance. The crucibles

were pre-cleaned in 5% nitric acid in a sonic bath for 20 min, rinsed 3 times in de-ionized water and dried overnight in an oven (60 °C). Each weighted sample was transferred in a conical base borosilicate vial capped with a septum. The vials were pre-cleaned using the same technique as that described above for the crucibles. The samples were placed in a heated rack at 90°C for one hour prior to analysis. Samples were analysed using a Micromass Isoprime universal triple collector IRMS in Dual Inlet mode coupled to a MultiCarb system in Geotop laboratories, UQAM. For each sample three drops of orthophosphoric acid ($\rho = 1.92$ g/cm^3) were delivered under vacuum. The resulting CO_2 was trapped in a cold finger at −180°C (liquid nitrogen) for 10 min. A water trap (−70°C) condensed moisture between the vial and the cold finger. The CO_2 was then heated at −60°C and focused in a second cold finger at −160°C for 5 min. The resulting gas was finally released in a fixed volume and the pressure of the reference gas was equilibrated with that of the sample. The monitoring gas is a Jackson Dome CO_2 with a $\delta^{13}C$ of −3‰ VPDB and a $\delta^{18}O$ of 25.8 ‰ VSMOW. For each analytical sequence reference materials were interspersed with the unkowns for normalization on the VPDB and VSMOW scales. The reference materials used are: (1) 'UQ6' calcite, with $\delta^{13}C = +2.25$ ‰ VPDB and $\delta^{18}O = +29.47$ ‰ VSMOW; (2) NBS18 calcite, with $\delta^{13}C = -5.01 \pm 0.03$ ‰ VPDB and $\delta^{18}O = +7.19 \pm 0.23$ ‰ VSMOW; and (3) an 'in-house' Mt. St-Hilaire, gem-quality magnesian-ankerite crystal with $\delta^{13}C = -5.61 \pm 0.07$ ‰ VPDB and $\delta^{18}O = 18.66 \pm 0.19$ ‰ VSMOW.

3.4. Trace element data

Trace element concentrations were measured using a laser ablation ICPMS system in the Geotop laboratories at UQAM. The system consists of a Photon-machines Analyte.193 G2 Pulse Excimer laser and a Nu Instrument Attom, high resolution, sector field ICPMS. The system was monitored using NBS610 glass standard and the carbonate samples were quantified using a USGS MACS3 LAICPMS calcite standard as internal standard. All samples were previously analyzed for major elements using the electron microprobe so Ca (or Mg in the case of siderite) was used as internal standards.

4. Results

4.1. Observational features

The massive carbonatite (Fig. 2a) is cut by sub-millimeter-scale whitish veinlets of calcite and brownish veinlets of Mg-ankerite. Between these veinlets, ghost phenocrysts of calcite and interstitial matrix are cut by myriads of micron-scale veinlets of undifferentiated carbonates, pervasively altering the rock to what has become a part magmatic, part-carbothermal carbonatite.

The silicocarbonatite (Fig. 2b) consists of mixed bands and patches of carbonatite and ultramafic silicate rock. Magmatic carbonates are calcite whereas late veinlets contain magnesian-ankerite. The carbonatite itself as well as the ultramafic rock are metasomatized and display pervasive carbonatation, sodic and potassic fennitization (albite and microcline) and oxidation to magnetite with subsequent hematite exsolution. The contacts between both lithologies are curved and appear ductile so they appear to have been comagmatic. Microscopic observations show traces of carbothermal fluids penetrating the ultramafic rock.

The alkaline lamprophyre (monchiquite; Fig. 2c) is an ultramafic panidiomorphic rock containing olivine globules partly replaced by calcite and biotite partly replaced by chlorite. Magnetite is mainly present as microlites but also present as phenocrysts. The olivine pseudomorphs contain calcite whereas the matrix' and veinlet's carbonates are ferroan-dolomite. The matrix carbonate may be magmatic and/or carbothermal. This lamprophyre is late and crosscuts all other lithologies at Lac Shortt.

The hornblendite (Fig. 2d) is also an ultramafic, porphyritic, hydrated rock. It consists of hornblende and appears to contain magmatic calcite but was pervasively carbonatized and thus also contains secondary, carbothermal calcite.

The dioritic sill (Fig. 2e) is highly metasomatized, shows early fennitization (albite and microcline), secondary pervasive carbonatation and hematization, and tertiary carbonatation-sulfidation in the form of whitish carbonate veinlets with coarse, fresh pyrite.

The mafic sill (Fig. 2f) is a highly metasomatized albite-biotite-carbonate-rich rock. Albite and biotite respectively represent sodic and potassic fennitization, to varying degrees, that appears to have been accompanied by carbonatization. Oxidation to magnetite is partly obliterated by late sulfidation to pyrite. Drusic quartz indicates open space crystallization and suggests shallow emplacement.

The syenite (Fig. 2g) consists of microcline and red hematite in a calcite and magnesian ankerite matrix, cut by a first generation of quartz-feldspar veinlets and a second generation of undifferentiated carbonates. Fennitization of the syenite probably introduced the potassium to make microcline so it is unclear if the syenite was originally a magmatic syenite (*sensu stricto*). Metasomatism of the syenite and the formation of veinlets of quartz and feldspars preceeded the carbonatization. Drusik textures associated with the silicate veinlets indicate open space cristallization and suggest shallow emplacement depths.

The ore is divided into low (Fig. 2h; 3–6 g/t) and high (Fig. 2i; up to 15 g/t) grades (Morasse, 1988). The dominating facies of the low grade ore, termed 'creamy carbonate' was first pervasively carbonatized and oxidized to hematite and subsequently sulfidized to auriferous pyrite. The high grade ore is 'brick-red' and was fennitized to microcline, carbonatized to mostly ferroan dolomite but with some magnesian-ankerite, oxidized to hematite, silicified and subsequently sulfidized with auriferous pyrite.

4.2. Major and minor element compositions

Out of the 75 carbonate samples analyzed for major and minor element concentrations (Table A1; Fig. 3), 35 are calcites, 32 are ferroan-dolomites, 6 are magnesian-ankerites and 2 are siderites. On a 100 % cation basis, calcites have Mg varying from about 0.02 to 2 atom. % and Fe from about 0.1 to 5 atom. %, dolomites have Mg from 16 to 28 atom. % and Fe from 12 to 29 atom. %, ankerites have Mg from 12 to 14 atom. % and Fe from 35 to 38 atom. % and siderites have Mg from 3 to 5 atom. % and Fe from 94 to 96 atom. %. Dolomites have Ca from 54 to 60 atom. % and ankerites have Ca from 49 to 51 atom. % (Table A1). Carbonatites contain calcite, dolomite and ankerite; lamprophyres contain calcite and dolomite; hornblendites contain only very pure calcite; mafic sills contain calcite and dolomite; dioritic sills contain dolomites and siderites; syenites contain calcite, dolomite; and ankerite and ore contain dolomite and ankerite (Fig. 1).

Carbonatites and silicocarbonatite have matrix calcite, white calcite veinlets and/or dykelets and brown dolomite and ankerite veinlets (Table A1). Lamprophyres have calcite globules and Mg-rich (Fe-poor) dolomite veinlets and matrix. The hornblendites only have very pure calcite with Mg <0.1 atom.% and Fe <0.2 atom.%. Mafic sills have calcite and dolomite veinlets and dolomite in the matrix. The dioritic sills have dolomite and siderite in the matrix, and dolomite-only veinlets. Syenites have calcite and dolomite both in the matrix and as veinlets. Finally, the ores host dolomite and ankerite but displays no calcite nor siderite. In general, carbonates that are magmatic (in carbonatite matrix, carbonatite injection in syenite and silicocarbonatite) are calcites and carbothermal phases can be either calcite, ankerite or dolomite. Ankerite is found only as brownish veinlets in carbonatite, syenite and ore. All carbonates are Sr-rich, with electron microprobe values ranging from below the limit of detection of about 380 ppm, to about 1.8 wt. %. Rubidium is below the limit of detection of 100–400 ppm and Ba is below the limit of detection of 410–450 ppm.

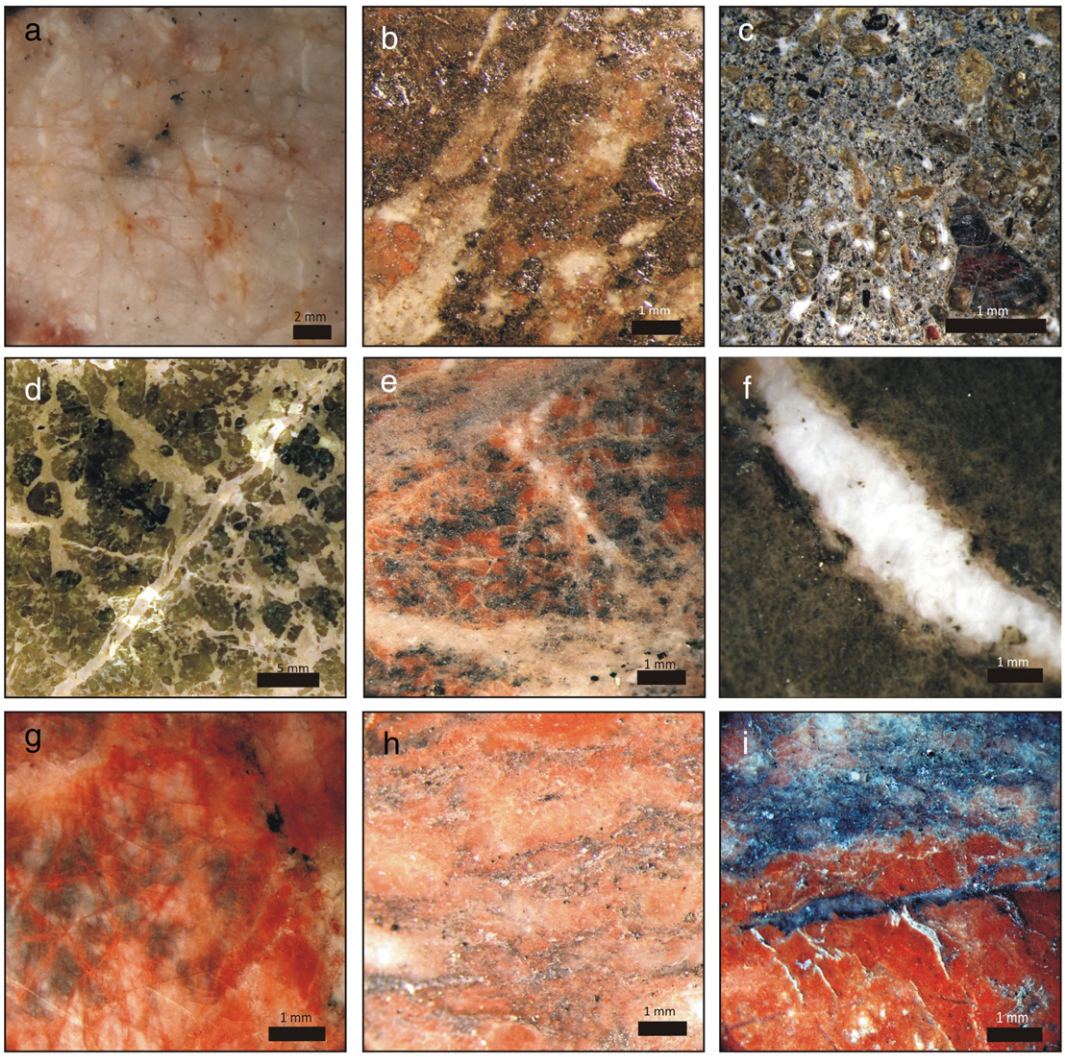

Fig. 2. Microscopic photographs and descriptions of the main lithologies of Lac Shortt magmatic-hydrothermal complex. (a) Carbonatite showing the whitish matrix filled with myriads of submillimetric carbonate veinlets, small brownish veinlets and patches, white N-S veinlets, galena (larger) and magnetite (small black specks). (b) Silicocarbonatite made of mixed bands and pockets of carbonatite and ultramafic silicate rock. The carbonatite is made or coarse calcite with biotite, feldspars, quartz and pyrite. The ultramafic silicate rock is made of course, partly chloritized biotite, magnetite with hematite exsolution quartz and feldspars. Late magnesian-ankerite veinlets cut through both lithologies. The ultramafic rock is pervasively carbonatized, albitized, oxidized to magnetite and has metasomatic K feldspar. (c) Alkaline lamprophyre (monchiquite) showing pseudomorphosed phenocrysts of former olivine now recrystallized to calcite, magnetite and quartz and partly chloritized phenocrysts of biotite in a matrix of ferroan-dolomite, magnetite-ilmenite. The sample is pervasively carbonatized. (d) Photograph of a polished section of the rock. Hornblendite (or calc-alkaline lamprophyre; vogesite or spessartite) showing porphyritic hornblende and apatite in a matrix of fine to medium grained calcite, with traces of pyrite and hematite. The rock is brecciated by numerous veinlets/dykelets of calcite. (e) Dioritic sill showing early red oxidation, later carbonatation (top left) and late carbonatation (white veinlets). The red areas contain microcline, albite and quartz. The black minerals are hematized magnetite. (f) Mafic sill with extension 'en echelon' veinlets/dyklets of calcite and magnesian-ankerite. The mafic sill contains plagioclase, undifferentiated carbonate, chloritized biotite, quartz and magnetite. The shear veinlets/dyklets consists of coarse calcite, drusik quartz and pyrite. (g) Syenite showing massive, brick-red microcline with myriads of red specks of hematite giving it its red color. The rock is pervasively carbonatized with a matrix of calcite and magnesian-ankerite, and is cut by veinlets of quartz-feldspar which are in turn cut by undiffentiated carbonate veinlets. The quartz-feldspar veinlets display open space crystallization textures. (h and i) The ore is divided into two types: low (h) and high (i) grade. The low grade ore (h) displays two alteration facies: (1) creamy carbonate and (2) the brick-red syenite. The creamy carbonate is pervasively carbonatized and oxidized to hematite. Some pyrite and quartz overprint this alteration. The brick-red syenite facies is present also in the high grade ore (i). It contains hematized microcline and quartz, is not magnetic, and displays pervasive carbonation, silicification and late sulfidization with gold-rich, coarse and euhedral pyrite. It is cut by late veinlets of quartz and hematite without pyrite. The protolith appears to be the syenite.

4.3. Strontium isotopic ratios

Carbonates incorporate very high amounts of Sr (average 5408 ± 3925 ppm, min. 761 ppm, max. 1.84 wt.%) and negligible amounts of Rb (Table A1) such that the mesured $^{87}Sr/^{86}Sr$ ratios can be assumed to be their initial ratios (Fig. 4; Table 1). Although carbonates may recrystallize and re-equilibrate at low temperature conditions, the Sr and C in carbonate isotopic systems, unlike that of oxygen will be more resistant to weathering and metamorphism and retain their original values (Kerrich et al., 1987). Lac Shortt $^{87}Sr/^{86}Sr$ values for carbonates show values very close to the 2.7 Ga depleted mantle (0.700–0.701) and thus appear to have retained their original Sr signatures. Initial Sr ratios ($^{87}Sr/^{86}Sr_0$) of carbonates in carbonatite (magmatic and carbothermal), mafic and dioritic sill white veinlets, coarse ankerite crystals in syenite and high and low grade ores all cluster tightly around depleted mantle values, ranging from 0.701297 ± 0.000007 to 0.701829 ± 0.000017. Carbonates in the syenites veinlets and in lamprophyres globules and veinlets have slightly more radiogenic values, ranging from 0.70259 ± 0.00003 to 0.70293 ± 0.00002). These results support previous work (Morasse, 1988; Prud'homme, 1990; Brisson, 1998) stating that the lithologies described above were co-magmatic and strongly suggest that they were derived from the depleted mantle.

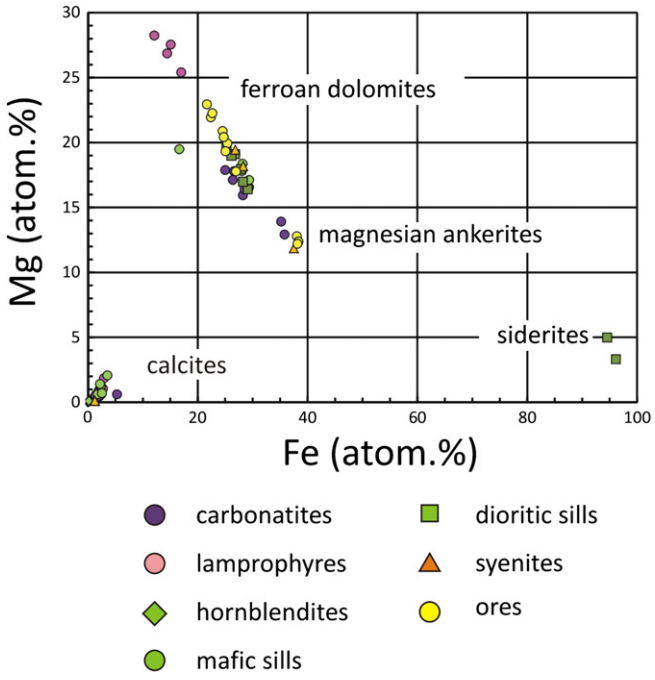

Fig. 3. Mg-Fe plots (in cation basis atomic %) of carbonate minerals at Lac Shortt, showing calcite, ferroan-dolomite, magnesian-ankerite and siderite for all the lithologies at Lac Shortt.

4.4. Stable isotopes

At Lac Shortt, $\delta^{13}C$ values from carbonates in carbonatites (including data from See, 1994) range from −5.94 to −2.62 ± 0.07 ‰ VPDB and mafic sills, lamprophyres and syenites have $\delta^{13}C$ values fall within the same range. The ores have the heaviest C isotope ratios ranging from −2.38 to −1.86 ± 0.07 ‰ (Fig. 5; Table 1). The $\delta^{13}C$ values at Lac Shortt extend from mantle-like (−5‰) to heavier values and exceed the −8 to −4 range of mantle carbonatites (Bell, 1989). The $\delta^{18}O$ in carbonates extend from 8.28 ± 0.19 ‰ VSMOW, within the carbonatite box (Bell, 1989), to 15.02 ± 0.19 ‰ VSMOW, outside the carbonatite box (Fig. 5, Table 1). Combined $\delta^{18}O$ and $\delta^{13}C$ (‰ VSMOW and VPDB, respectively) values for all lithologies range from mantle-like values ($\delta^{18}O = 8$, $\delta^{13}C = -6$) and extend towards heavier O and C isotopic ratios along a concave-upward curve (Fig. 5) with the exception of one carbonatite and one lamprophyre data point. The ores lie at the heavy end of the curve, suggesting hydrothermal altered values, in agreement with the hydrothermal nature of the ore.

4.5. Incompatible element compositions

Trace elements were analyzed in carbonates from all lithologies present at Lac Shortt (Table A2). Incompatible element concentrations are plotted on spidergrams normalized to depleted mantle (MORB) composition (Sun, 1980; Saunders and Tarney, 1984; Fig. 6). Trace elements are divided into incompatible and mobile (Sr, Ba), ultra-incompatible and immobile (Th, U, Ta, Nb), generally incompatible and immobile (Zr, Ti and REE) and incompatibility increases towards the actinides (towards Th for mobiles (Sr, Ba) and towards U for HFSE and REE. The spidergrams display some of the REE, although REE are shown in greater details in Fig. 7. A few datapoint connecting lines are given for selected samples but could not be given for all because analyses were commonly below limits of detection, especially for actinides (Th, U) and HFSE (Ta, Nb, Zr, Ti). Lines are dashed when points are missing because concentrations are below limits of detection. The full range of trace element concentrations is delineated by a gray envelope which is superimposed by the yellow envelope of ore carbonates, for comparison. Generally, trace element patterns for carbonates from all lithologies are very similar to carbonates from the ores.

Compared to the depleted mantle, carbonatite carbonates (Fig. 6a) are enriched in Sr and REE, have intermediate concentrations of Ba

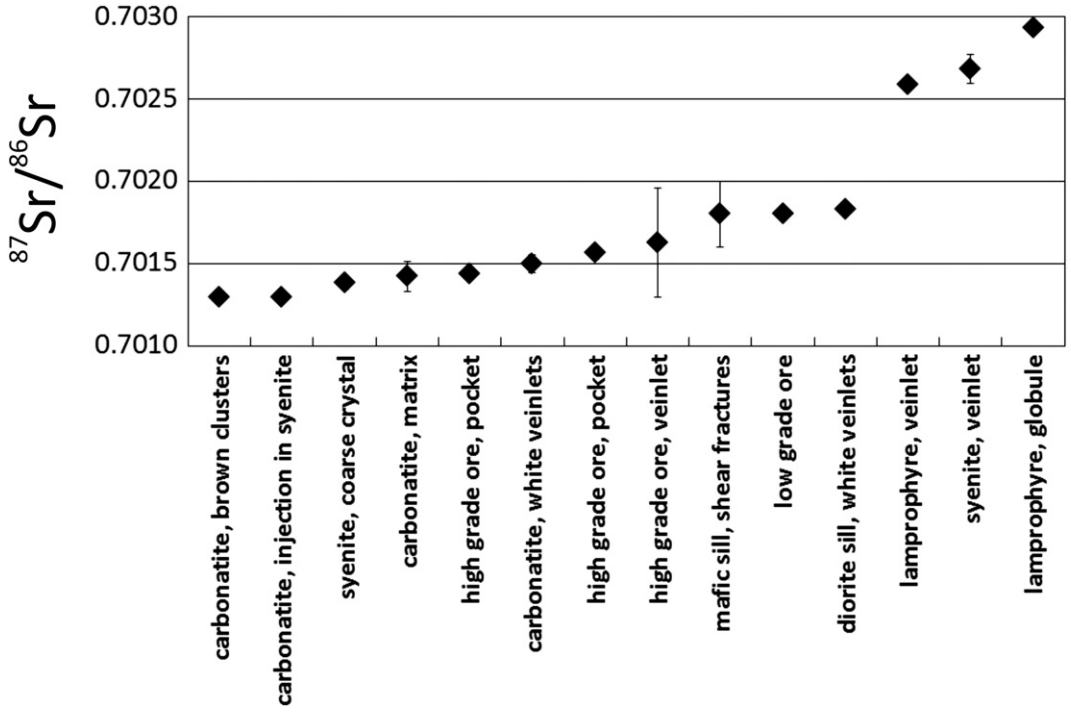

Fig. 4. $^{87}Sr/^{86}Sr_0$ isotope ratios from carbonates from each of the lithologies at Lac Shortt. 2σ standard error bars are smaller than the symbols where not shown. Carbonates from the carbonatites, the syenite, the ore the mafic and the dioritic sills display tightly clustered values plotting very close to the 2.7 Ga depleted mantle values (approximately 0.701). Syenite veinlet and the lamprophyre carbonates have somewhat more radiogenic values (0.70259–0.70293) and only low grade ore ankerite has a more radiogenic value of 0.7097. It is striking that carbonatite (magmatic and carbothermal), coarse calcite crystal in syenite and high grade ore cluster tightly around 0.7013–0.7016 ± 0.000007–0.0003.

Table 1
Strontium, carbon and oxygen isotopic compositions of carbonate minerals at Lac Shortt. 'Cc' stands for calcite, 'Dol-Fe' and 'Ank-Mg' stand for ferroan-dolomite and magnesian-ankerite, respectively. 1σ standard deviations are ±0.07 ‰ and ±0.19 ‰ for $\delta^{13}C$ and $\delta^{18}O$, respectively.

Rock #	Lithology, material	Mineral	$^{85}Rb/^{86}Sr$	$^{87}Sr/^{86}Sr$	2σ error	$\delta^{13}C$ vpdb	$\delta^{18}O$ vsmow
LS8547	Carbonatite, brown veinlet with some matrix	Ank-Mg	0.000003	0.701297	0.000007	−3.60	12.53
LS85110B	Carbonatite, injection in syenite	Cc	0.00000	0.70130	0.00001	−4.04	12.35
LS8621	Syenite, coarse white crystal	Ank-Mg	0.00006	0.70138	0.00004	−2.96	12.50
LS8547.2	Carbonatite, matrix	Cc	0.00006	0.70142	0.00009	−4.89	14.32
LS8534B	High grade ore, veinlet	Dol-Fe	0.00002	0.70144	0.00003	−2.33	13.15
LS8547.3	Carbonatite, white veinlet	Cc	0.00901	0.70150	0.00005	−3.08	12.98
LS8534B.2	High grade ore, veinlet	Dol-Fe	0.05411	0.70156	0.00004	−2.32	13.10
LS8534A	High grade ore, veinlet	Dol-Fe	0.00015	0.70163	0.00033	−2.38	12.92
LS8554	Mafic sill, shear veinlet	Dol-Fe	0.00059	0.7018	0.0002	−5.41	11.01
LS8584B	Low grade ore, veinlet	Ank-Mg	0.00040	0.70180	0.00001	−1.86	12.22
LS8671A	Dioritic sill, white veinlet	Ank-Mg	0.000022	0.701829	0.000017	−2.69	12.47
LS8552	Lamprophyre, veinule	Dol-Fe	0.00001	0.70259	0.00003	−3.48	13.35
LS8621.2	Syenite, veinlet	Ank-Mg	0.00010	0.70268	0.00009	−3.64	12.43
LS8552.2	Lamprophyre, globule	Cc	0.00004	0.70293	0.00002	−4.00	15.02

and are depleted in immobile Th-U-Ta-Nb-Zr-Ti. Carbonates from carbonatites have concentrations of Sr-Ba-Th-U-Ta-Nb-Zr-Ti strikingly similar to those of the ores, and concentrations of REE higher than those of the ores by 1–1.5 orders of magnitude. Silicocarbonatite (Fig. 6b) carbonates display a behavior similar to those of carbonatites but have somewhat higher concentrations of Nb and LREE (La-Ce-Nd). Lamprophyre (Fig. 6c) carbonate trace elements range widely in concentration, have U-Th below limits of detection (0.01 and 0.04 ppm, respectively; Table A2), generally have HFSE and Y negative anomalies and LREE-enriched patterns. Lamprophyre carbonates have incompatible-mobile elements (Sr-Ba), actinides (U-Th), ultra incompatible elements (Ta-Nb-Zr-Ti) very similar to those of the ores and are LREE-enriched compared to ore carbonates. The laser might have intercepted zircon nanocrystals in one Zr-rich analysis. Carbonates from the 3 mafic lithologies (Fig. 6d), especially those of the dioritic sill, are strikingly similar to ores carbonates. They are enriched in Sr-Ba, show gradual depletion in Th-U-Ta-Nb-Zr-Ti and have convex-upward, LREE-enriched REE patterns. Calcites in hornblendites have relatively low incompatible element concentrations compared to other lithologies and are very pure (Fig. 3). Syenite carbonates (Fig. 6e) were commonly below the detection limits, which limits comparison and interpretation. They nevertheless show concentrations of Sr-Ba, U and REE which are very similar to those of ore carbonates.

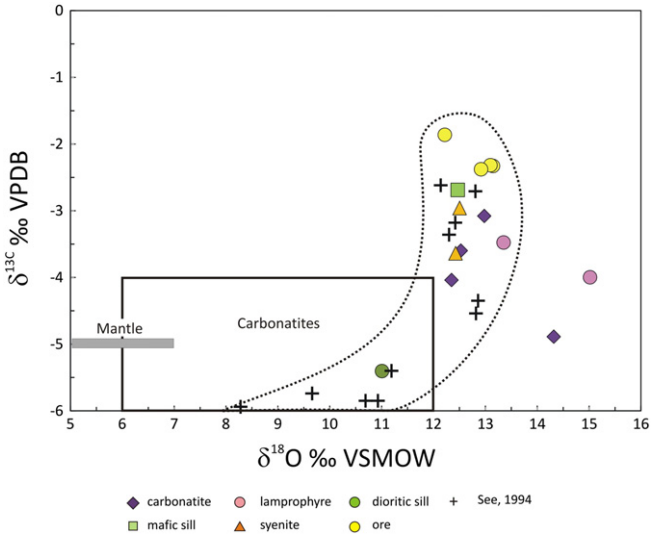

Fig. 5. $\delta^{13}C$ vs $\delta^{18}O$ plot for Lac Shortt samples (‰ VPDB and VSMOW, respectively). Mantle and carbonatite boxes are from Kerrich et al. (1987), Keiser (1986) and Bell (1989). Increasing fluid/rock ratio envelope is discussed in the text. 1σ standard deviations are ±0.07 ‰ and ±0.19 ‰ for $\delta^{13}C$ and $\delta^{18}O$, respectively, and are smaller than the symbols.

Ore carbonates (Fig. 6f) have positive Sr-Ba anomalies, actinides and HFSE often below limits of detections, negative Ti anomalies and MORB-like, flat REE patterns with mild positive to negative slopes.

4.6. Rare earth elements patterns

Chondrite normalized REE patterns are plotted separately for carbonates from each comagmatic lithology present at Lac Shortt. Emphasis is put on comparison of all carbonates REE patterns to those of the ores (yellow envelope) and on the four tetrads. (i.e., features whereby REE patterns are divided into 4 groups of 3-4 elements that appear to behave independently from each other; e.g., Monecke et al., 2002; Veksler, 2005) (T1–T4; Fig. 7). Given that numerous datapoints had concentrations below the limit of detection, it was not possible to plot meaningful continuous lines through concentration points, although a few were drawn for each diagram to highlight the patterns where definable. A light gray envelope was drawn to show the extent of all datapoints within specific lithologies, and these gray envelopes are superimposed by the ore's yellow envelopes for comparison.

Most carbonates have a narrow range of HREE (Ho, Er, Tm, Yb, Lu) in the 4th tetrad, usually ranging between 10 and 100 times chondrite, but vary greatly in terms of MREE (Sm, Eu, Gd, Tb, Dy, Y) and LREE (La, Ce, Pr, Nd) resulting in carbonates plotting in two populations: LREE-enriched (LREE up to 4000 × chondrite) or flat REEs (LREE 10–100 × chondrite). Very few carbonate plot lower than the flat-REE population and are REE-depleted (LREE 1–10 × chondrite). Tetrad effects are well developed for some lithologies: Tetrad T1 (La, Ce, Pr, Nd) is similar for carbonatite, silicocarbonatite, some lamprophyre and syenite, and is convex upward and split into high LREE/negative slope and low LREE/positive slope. Tetrad T2 (Sm, Eu, Gd) is not as well defined, mostly because Sm was commonly below the limits of detection. The two distinct higher and lower LREE populations plot closer to each other and cannot be easily distinguished with T2 REEs. Tetrad T3 (Tb, Dy, Y, Ho) is similar for most lithologies and display negative slopes and are usually concave upward. Yttrium reaches high concentrations (average of 83 ppm; maximum of 288 ppm; Table A2) and is thus highly reliable while Holmium is commonly below the limit of detection. The two higher and lower REE populations can be distinguished within carbonatites, silicocarbonatites and mafic lithologies (mafic and dioritic sills and hornblendites; Fig. 7d). Tetrad T4 (Er, Tm, Yb, Lu) is most depleted and shows both positive or negative slopes. Overall, the higher and lower REE populations appear distinctly for silicocarbonatites, syenite and for the mafic and dioritic sills. Within the carbonatite, the matrix and the white veinlets have high REE while the brown veinlets and the carbonatite injection in syenite have lower REE patterns. These higher and lower REE populations are also present for the silicocarbonatite although magmatic and hydrothermal carbonates

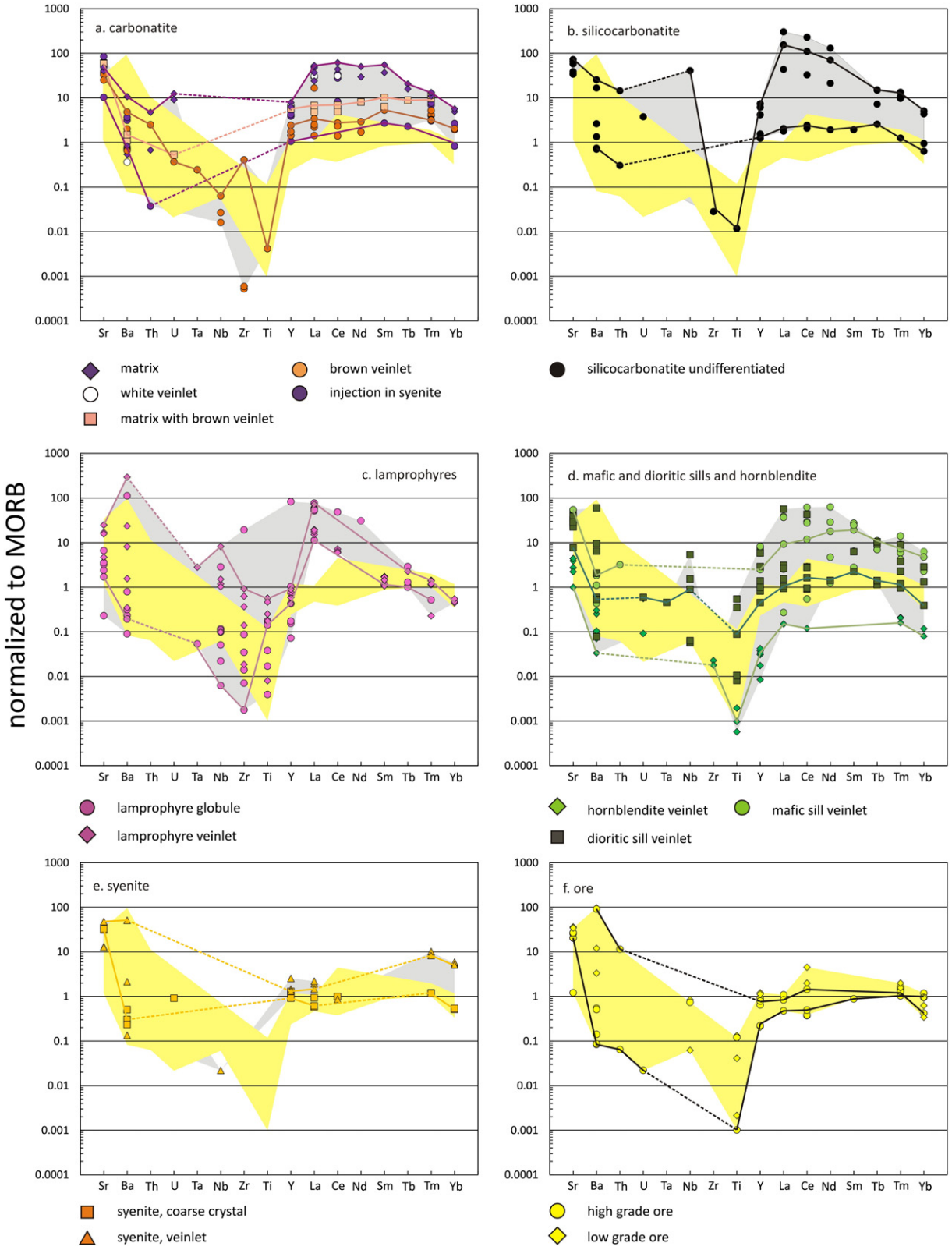

Fig. 6. Laser ablation ICPMS, depleted mantle-normalized incompatible element spidergrams for carbonates from Lac Shortt. (a) carbonatites; (b) silicocarbonatites; (c) lamprophyres; (d) mafic and dioritic sills and hornblendite; (e) syenites (f) ore. Among the incompatible elements, Sr and Ba are mobile, Th-U-Ta-Nb-Ti are incompatible and immobile and REE are generally incompatible and may be mobile. MORB data from Saunders and Tarney (1984) and Sun (1980). The gray envelopes delineate all datapoints and are superposed by yellow envelopes, which are from ore carbonates, shown for comparison. Datapoints are connected by lines where possible, to show general patterns.

could not be distinguished. In the syenite, all veinlets have low REE and the coarse ankerite crystal has both high and low REE signatures. The ore has a low REE signature similar to that of the brown veinlets in the carbonatite, the carbonatite injection in syenite, the lower REE population of the silicocarbonatite and the syenite veinlets, with nearly flat but overall concave upward patterns.

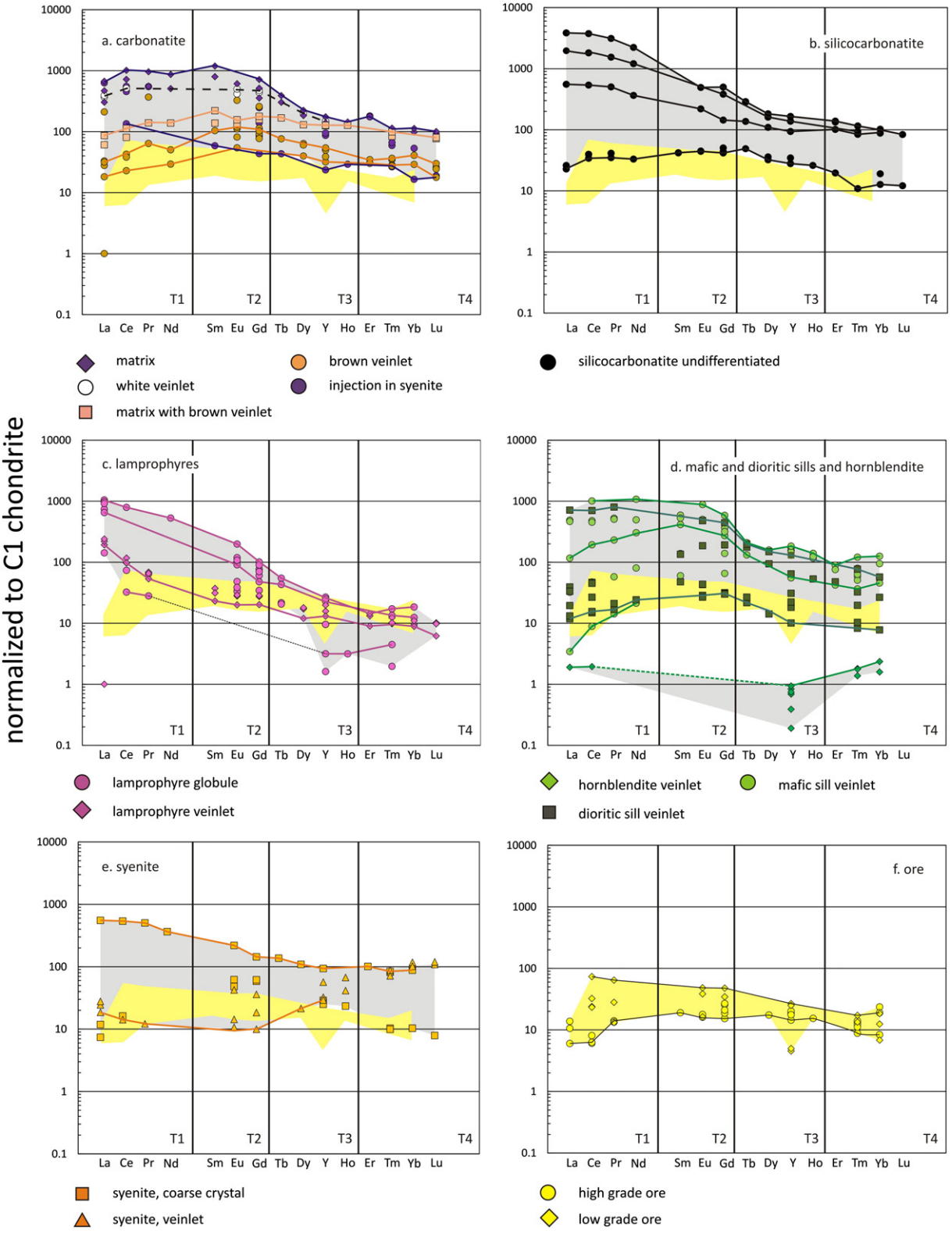

Fig. 7. Laser ablation ICPMS, rare earth element patterns normalized to C1 chondrite for carbonates from Lac Shortt. (a) carbonatite; (b) silicocarbonatite; (c) lamprophyres; (d) mafic and dioritic sills and hornblendite; (e) syenite; and (f) ore. Rare earth elements include the lanthanides and yttrium, and are divided in terms of tetrads (T1–T4). Chondrite data are from Sun (1980). The gray envelopes delineate all datapoints and are superposed by yellow envelopes, which are from ore carbonates, shown for comparison. Datapoints are connected by lines where possible, to show general patterns.

Chondrite-normalized, rare earth element concentrations from Lac Shortt bulk rocks (carbonatite dikes and intrusions, alkaline, calc-alkaline and ultramafic lamprophyres, dioritic sills, syenite dikes, syenite shreds in carbonatite and high grade ore) display chondrite-normalized patterns broadly similar to those of the carbonates, with relative LREE enrichment, but with the carbonatites being more REE enriched, the lamprophyres, syenite and ore having moderate relative enrichments, and the dioritic sill being the most REE depleted (Fig. 8;

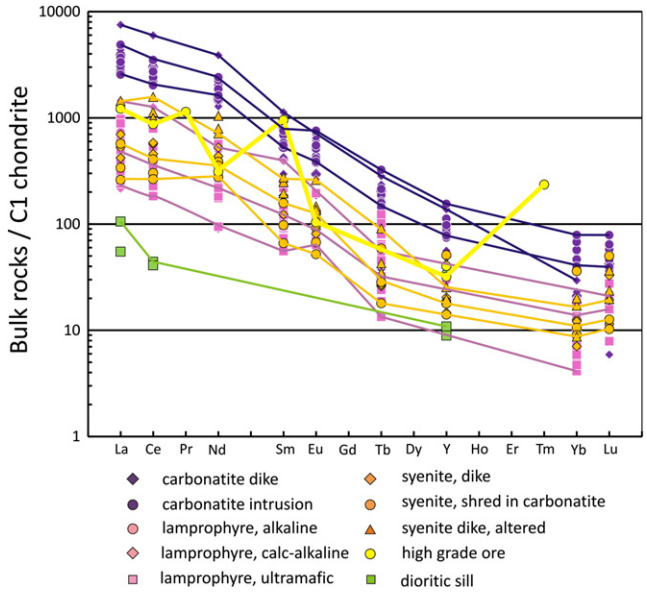

Fig. 8. Lac Shortt bulk rock REE patterns. Data are from Morasse (1988), Prud'homme (1990), Bourne and Bosse (1991) and Brisson (1998). Results are normalized to chondrite and plotted in log scale.

Prud'homme, 1990; Bourne and Bosse, 1991; Brisson, 1998; Morasse, 1988). Carbonatites have the greatest LREE enrichment with La/chondrite ranging from about 2200–7800. Lamprophyres and syenites have similar LREE enrichments with La/chondrite ranging from 200 to about 1000. Praseodynium, Gd, Dy, Ho, Er and Tm are always below the limit of detection (except for two data points). High grade ore has one sample with positive Sm, Pr and Tm anomalies compared to other bulk rock analyses.

The bulk carbonatites (dykes and other intrusions) are highly enriched in LREE, with La/chondrite ≈ 2000–8000, and have strongly negative REE slopes, with La/Lu ≈ 3000–400 (Table A3; Fig. 8). The bulk lamprophyres (alkaline, calc-alkaline- and ultramafic) are LREE-enriched, with La/chondrite ≈ 200–1000 and La/Lu ≈ 200–700, whereas lamprophyre veinlets have a smaller LREE-enrichment. The bulk syenites have moderate to strong LREE-enrichment. By comparison to bulk rocks, carbonates from syenites are bimodal and have both higher and lower LREE enrichments. Finally, the bulk ore is much more enriched in LREE than carbonates from the ore, which have flat REE patterns. Syenites have REE patterns very similar to lamprophyres, with La/chondrite ≈ 200–1000 and La/Lu ≈ 50–600. The Bulk ore (high grade), has REE pattern similar to lamprophyres and syenites, with La/chondrite ≈ 1000 but Lu below detection limit. However, the single bulk ore analyses with most REE above detection limits displays a sawtooth pattern with negative Nd and positive Pr, Sm and Tm anomalies. Bulk dioritic sill has very low REE concentrations, with La/chondrite around 100 and a negative slope similar to other bulk rocks. In general, bulk rock REE patterns support the fact that all lithologies and ore are cogenetic.

5. Discussion

5.1. Relations amongst gold, syenites, lamprophyres and carbonatites

Pye (1976) first noted a temporal association between gold and lamprophyre dykes while observing lamprophyre dykes cutting through- and being cut by gold mineralization at the Pickle Lake gold camp, northwestern Ontario, Canada. Similar temporal relationships exist at Kirkland Lake, as reported for example by Parsons (1948), who described lamprophyres predating gold at the Bidgood mine and by Thomson (1950), who reported lamprophyre dikes postdating mineralization at La Macassa mine, Ontario. Smith (1986) also reported pre- to syn-mineralization lamprophyres in the Lake of the Woods region, Ontario, Canada. Numerous studies have considered the relationship between lamprophyres and gold deposits in Archean cratons such as the Yilgarn (Autralia) and the Superior (Canada) cratons (Rock, 1986, 1987; Rock et al., 1987; Rock, 1988; Rock and Groves, 1988a,b; Rock et al., 1988; Wyman and Kerrich, 1988; Rock et al., 1989; Rock, 1991). Rock et al. (1987) underlined that fresh lamprophyres contain abundant K_2O, Ba, Rb, H_2O, CO_2, S and F, the same elements that characterize the metasomatic alteration that is commonly associated with gold deposits (potassic alteration, high LILE signatures, carbonatation and sulfidation). Although lamprophyres are porphyritic and quenched at shallow depths, they sometimes carry mantle xenoliths and diamonds testifying that they originate at depths exceeding 130 km (Rock and Groves, 1988a,b). Rock et al. (1987) also reported that gold was systematically enriched in all lamprophyres, mineralized or barren. However, this was subsequently refuted by Wyman and Kerrich (1988) who suggested a sampling bias and argued that, although lamprophyres were spatially and temporally associated with major shear zones and gold mineralizing events, they are not enriched in gold and the emplacement of lamprophyre dike swarms does not represent a mineralization event. Jensen and Barton (2000) found that gold – syenite – lamprophyre associations are characterized by field relations that suggest that syenites and gold are contemporaneous and that lamprophyres intruded afterwards. However, the length of time that separates the gold-syenite system from the lamprophyres is generally unconstrained. In the example of the Murdock Creek syenite, Rowins et al. (1993) argued that lamprophyre magmas and the Murdock Creek syenite were coeval based on field relations and trace element geochemistry and U-Pb zircon ages for syenites and lamprophyres returned similar ages (ca. 2670-2680 Ma; Wyman and Kerrich, 1987, 1988; Corfu et al., 1989; Ben Othman et al., 1990). Gold mineralization has been found to be both contemporaneous with syenitic and lamprophyric magmatism and to postdate this magmatism, but the mineralization is always associated with the carbonatation that is in turn associated with this magmatism (Wyman and Kerrich, 1988; Rowins et al., 1993).

5.2. Strontium, C and O isotope ratios in Abitibi gold ores

Strontium isotope analyses in a variety of minerals from Abitibi gold deposits led Kerrich et al. (1987) to suggest a geographic variation in the Sr isotope ratios along the Cadillac-Larder Lake fault zone (CLL) with $^{87}Sr/^{86}Sr_0$ ratios of 0.703–0.704 around Val d'Or, 0.700–0.702 around Bourlamaque, 0.701–0.702 around Bousquet, 0.703 around Noranda, 0.701 around Kirkland Lake, and values ranging from 0.701–0.704 along the Destor-Porcupine fault zone (DP). For comparison, the depleted mantle at 2690 Ma, the time at which these deposits formed (Corfu, 1993), had a $^{87}Sr/^{86}Sr_0$ ratio of about 0.700–0.701 (Wilson, 1989). The $\delta^{13}C$ (‰ VPDB) values of Fe-Mg-Ca carbonates also showed geographic variation on an E-W trend from −6 to −8.5 at Malartic, −8 to −9 at Cadillac, −2 to −4.5 at Kirkland Lake and −0.5 to −3.5 at Timmins. These geographic variations were interpreted to reflect heterogeneities in the crust although the source of the solutes present in the metasomatized rocks of these faults remained unknown. The authors stressed that the Sr and C isotopic systems in the carbonates, unlike that of oxygen, were not disturbed by meteorization and metamorphism and appeared to have retained their original values. Although Kerrich et al. (1987) concluded that the solutes present in metasomatized shear zone rocks may originate from greenstone crustal rocks, Fyon et al. (1984) and Colvine et al. (1984) had previously concluded that CO_2 streaming through these faults represented fluids degassing from the mantle.

5.3. Solutes and mantle gold

The majority of the carbonates from Lac Shortt lie between 0.7013 and 0.7018 ± 0. 0001 and compare well with the ratios found in the

bulk rocks from Lac Short; 0.70125–0.70135 (Tilton and Bell, 1994). These values are very close to those of the depleted lithospheric mantle. Using Sr as a proxy for solutes in carbonatite magma and associated hydro-carbothermal fluids, and assuming gold and REE also behaved as a solutes in the system, gold/REE mineralization associated to magmatic and carbothermal carbonates from the carbonatite, silicocarbonatite, mafic and dioritic sills, syenites and ores appear to have originated from the sub-continental depleted mantle and suffered very little crustal contamination. Only 3 carbonates samples – one in a syenite veinlet and 2 in lamprophyres – have slightly more radiogenic Sr values, ranging from 0.7026–0.7029, and thus probably incorporated small amounts of crustal Sr. It is striking that the carbonatite, syenite and high grade ore all plot within a very narrow $^{87}Sr/^{86}Sr_0$ interval. We interpret this to result from the fact that they have a common origin, i.e., that carbo-hydrothermal gold was transported in a mantle-derived carbonatite volatile phase.

5.4. Solvents and hydrothermal alteration

The oxygen isotope system is generally very sensitive to down-temperature re-equilibration and alteration (Kerrich et al., 1987). The depleted mantle has a $\delta^{18}O$ value of about +5 to +7 ‰ VSMOW (c.f. Keiser 1986). The Lac Shortt oxygen isotope values for carbonates (this study) and bulk carbonatites (See, 1994) extend from +8, within the carbonatite box (Bell, 1989; Fig. 6), towards heavier, lower temperature and more altered values. The mafic sills have a carbonatite-like value of +11.01 ‰ and carbonatite, syenite and ore samples cluster from +12.22 to +13.15 ‰, apart from the carbonatite matrix which has of $\delta^{18}O$ value of +14.32 ‰. As illustrated by the lack of correlation between $^{87}Sr/^{86}Sr_0$ and $\delta^{18}O$ (not shown), the alteration process, witnessed by $\delta^{18}O$ values, is decoupled from the crustal contamination process, monitored using the Sr isotope. Another reason why the oxygen isotope system was open may be the non-respect of stoichiometry between $CO_3^{2-}{}_{(melt)}$, $CO_{2\ (fluid)}$ and $CO_3^{2-}{}_{(carbonate)}$. Although this trio has a carbon molar ratio of 1:1:1, oxygen, in turn has a molar ratio of 3:2:3. This implies that upon exsolution of CO_2 from the carbonatite melt, O^{2-} becomes available, and this could contribute to the oxidation of iron and hematization observed in the syenites and ores. When CO_2 precipitates CO_3^{2-} in carbonates, it must take up oxygen from its surroundings.

The carbon isotopic system is more robust to alteration and thus retains its original, magmatic hydrothermal values longer (Kerrich et al., 1987). Carbonates (this study) and bulk carbonatites (See, 1994) have $\delta^{13}C$ values which extend from mantle-like values of about −6‰ to heavier values, reaching about −2‰. These values are similar to those of other Abitibi gold ore deposits (Veizer et al., 1989a,b). However, at Lac Shortt, there appears to be a fractionation trend between lighter values for mantle-derived carbonatites and heavier values for hydro-carbothermal carbonates. Carbonatite samples range from −4.89 to −3.08, magmatic carbonate in syenite has a value of −2.96, the diorite veinlet has a value of −2.69, high grade ore ranges from −2.38 to −2.33 and the low grade ore has a value of −1.86‰ (Fig. 9b). The process which drives the $\delta^{13}C$ values from light values in magmatic carbonates to heavier values in carbothermal carbonates is also decoupled from the crustal contamination processes, as witnessed by the non-correlation of $\delta^{13}C$ and $^{87}Sr/^{86}Sr_0$ (not shown).

Combined carbon and oxygen isotopic ratios plot along a concave upward curve with initially increasing $\delta^{13}C$ and subsequently increasing $\delta^{18}O$ ratio (Fig. 5). This type of curve has been interpreted to result from increasing fluid/rock ratios for fluids with dominant CO_2 concentrations (Boulvais et al., 1998). It has also been interpreted to result from high temperature fractionation crystallization (Pearce et al., 1997; Bouabdellah et al., 2010), hydrothermal alteration (Andrade et al., 1999), crustal contamination and weathering (Bouabdellah et al., 2010). The strong correlation between $\delta^{13}C$ and $\delta^{18}O$, the poor correlation of $^{87}Sr/^{86}Sr_0$ with both $\delta^{13}C$ and $\delta^{18}O$ and the absence of a correlation between the $\delta^{13}C$ vs $\delta^{18}O$ trend and lithology types suggests that the $\delta^{13}C$ and $\delta^{18}O$ trend is the result of either hydrothermal alteration or increased fluid-to-rock ratios. The fact that ores have the

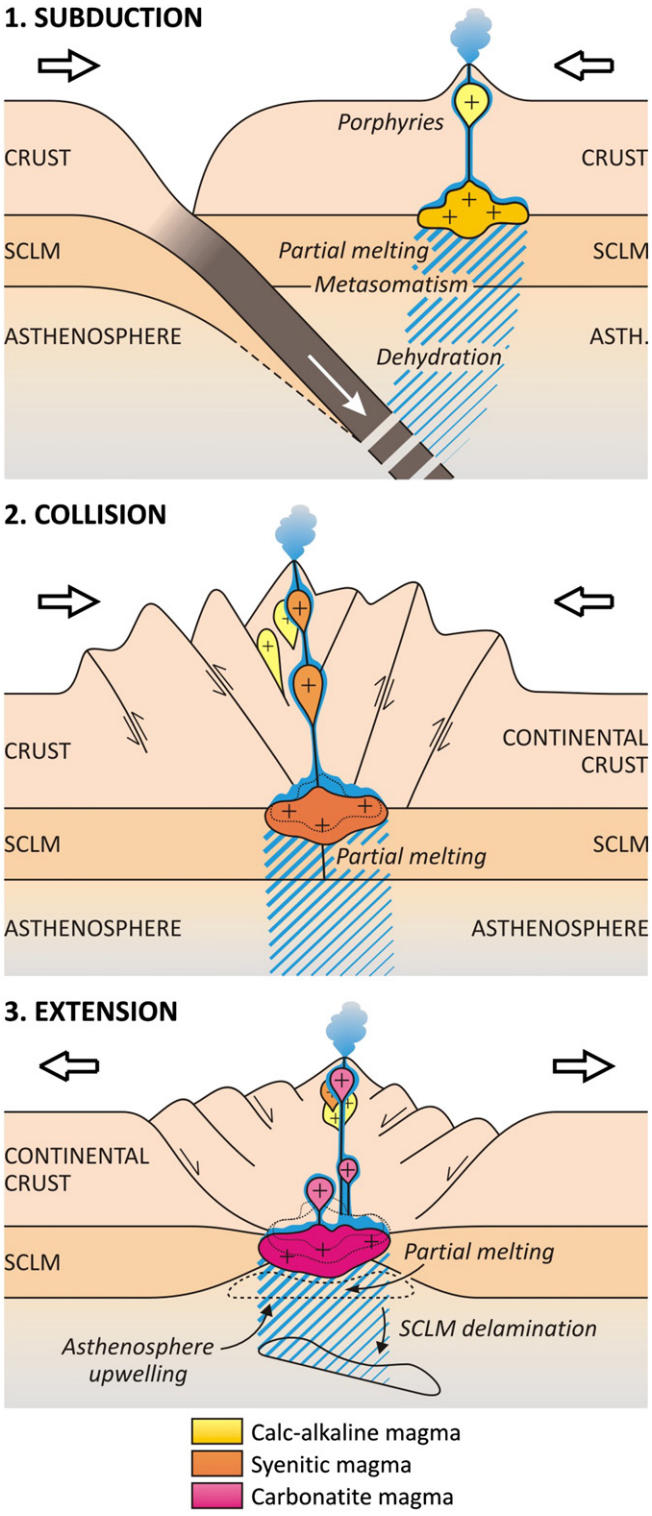

Fig. 9. Petro-metallogenetic model for Au-REE mineralization at Lac Shortt. The model is based on our data as well as on previous work on subduction-collision tectonics by Smithies and Champion (1999), Richards (2009), Eyal et al. (2010), Martin et al. (2012), Krystopowicz and Currie (2013), on isotope geochronology at Lac Shortt by Thorpe et al. (1984) and Morasse (1988), on Archean tectonics of Abitibi by Corfu et al. (1989), Corfu (1993), Mortensen (1993), Kerrich and Cassidy (1994), Mueller et al. (1996), and Ayer et al. (2002), and on the theses of Morasse (1988), Prud'homme (1990), See (1994) and Brisson (1998) on Lac Shortt.

heaviest $\delta^{13}C$ and $\delta^{18}O$ values (Fig. 5), and thus, the greatest fluid/rock ratio corroborates this interpretation. We propose that the solvents from which the carbonates precipitated were initially derived from the mantle at low fluid/rock ratios, and were gradually enriched in heavier crustal C and O through increasing fluid/rock ratios.

5.5. Trace element fingerprinting

Carbonates from Lac Shortt are enriched in incompatible-mobile LIL elements (Sr, Ba), depleted in incompatible-immobile elements (Th, U, Ta, Nb, Zr, Ti) and enriched in incompatible-mobile REE, compared to the depleted mantle and chondrites (Figs. 6–7). These signatures are consistent with the transport of the mobile elements by a carbo-hydrothermal fluid, and with the formation of the mineralization by metasomatic processes. Furthermore, the similarity of the trace element signatures of the gold ore and other lithologies is consistent with transport of the gold by a hydro-carbothermal fluid that was comagmatic with the mantle carbonatite, silicocarbonatite, mafic magmas and syenite. Focusing on the chondrite-normalized rare earth element patterns (Fig. 7), the carbonates plot as two distinct populations: one LREE-enriched and one with a flat REE pattern. The flat REE pattern is associated with the gold ore and is also found in some of the carbonatite, some silicocarbonatite, most dioritic sills and syenite's carbonates. Aqueous fluids can complex REE and carbonic fluids probably can transport REE complexes as carbonate species (Williams-Jones et al., 2012), and LREE are more compatible in carbonate minerals than MREE and HREE. The LREE-depleted patterns of ore and other contemporaneous lithologies thus probably result from preferential deposition of LREE-bearing minerals and gold in the ore. This is in agreement with bastnaesite, ancylite and synchysite identified at Lac Shortt (Morasse, 1988; Prud'homme, 1990).

5.6. Metallogenetic model

Syn-collisional magmatism is generally preceded by calc-alkaline magmatism and followed by alkaline magmatism (Eyal et al., 2010), extensional tectonics and sub-continental lithospheric mantle delamination (Smithies and Champion, 1999; Richards, 2009; Martin et al., 2012; Krystopowicz and Currie, 2013). Lead-Lead ages from galena returned 2680–2665 Ma for the syenite and 2652 Ma for carbonatite at Lac Shortt (Thorpe et al., 1984; Morasse, 1988). At that time in Abitibi, subduction and calc-alkaline magmatism had been replaced by late-Archean collisional orogenesis and mildly alkaline magmatism, and was gradually evolving towards post-collisional extensional and alkaline magmatism (Corfu et al., 1989; Corfu, 1993; Mortensen, 1993; Kerrich and Cassidy, 1994; Mueller et al., 1996; Ayer et al., 2002). The collision resulted in trans-lithospheric suture zones such as the well-known Cadillac-Larder Lake fault zone, the Lamarck shear zone and the Opawica Lake fault zone, present at Lac Shortt, in which the auriferous alkaline systems and gold deposits are hosted (Groves et al., 1998; Robert, 2001; Bigot, 2012). It is in this general context that Lac Shortt alkaline magmatic-hydrothermal activity took place.

Field relations (Morasse, 1988; Prud'homme, 1990; Brisson, 1998) as well as the lead-lead ages of 2680–2665 Ma obtained for the syenites and of 2652 for the carbonatites (Thorpe et al., 1984; Morasse, 1988) indicate that the carbonatite postdated syenitic magmatism. When integrated into the petrogenetic and tectonic evolution of Abitibi (Corfu et al., 1989; Corfu, 1993; Mortensen, 1993; Kerrich and Cassidy, 1994; Mueller et al., 1996; Ayer et al., 2002), it appears that the syenitic and carbonatitic magmatism followed calc-alkaline magmatism. This, along with petrographic observations, lithogeochemical and isotopic analyses from previous studies (Bourne and Bosse, 1991; See, 1994) and the present paper allows us to propose a petro-metallogenetic model for the gold and REE mineralization at Lac Shortt (Fig. 9). In this model, the mafic, calc-alkaline magmas (mafic and dioritic sills) originated from the continental arc magmatism and the metasomatized, late-Archean sub-continental depleted mantle. These magmas were gradually replaced by mildly alkaline, syenitic magmatism and hydrothermalism during the late-Archean collisional orogeny. Collision and extensional relaxation is typically followed by subcontinental depleted mantle delamination (Smithies and Champion, 1999; Richards, 2009; Martin et al., 2012; Krystopowicz and Currie, 2013). This type of extensional regime was identified specifically at Lac Shortt (Brisson, 1998) as well as more generally in the area (Corfu et al., 1989; Corfu, 1993; Mortensen, 1993; Kerrich and Cassidy, 1994; Mueller et al., 1996; Ayer et al., 2002). At Lac Shortt mantle-derived carbonatitic magmatism accompanied the extensional period. We suggest the carbonatite magma and its mantellic roots must have became saturated with a Au-REE-bearing, hydro-carbothermal fluid and increasing circulation of this fluid through the Lac Shortt lithologies eventually raised the fluid/rock ratio (Fig. 6) pumping Sr, REE and gold from the mantle.

Lac Shortt bulk carbonatite was reported to have between below the detection limit of 0.01 ppm and 0.8 ppm Au (Prud'homme, 1990). We calculated that a carbonatite with 0.5 ppm Au would have to weigh 24.8 Mt, i.e., equivalent to a cube of a side of 200 m at a density of 2.711 g/cm^3, to host the 12.4 tons of Au reported to have been extracted from Lac Shortt ore (Brisson, 1998), which is a reasonable mass/size for a carbonatite. Furthermore, we stress that it is the whole carbonatite system, rooted into the depleted mantle, that is suggested to have provided the Au-bearing, carbo-hydrothermal fluid, and not just its surface expression.

6. Conclusions

Field relations as well as isotopic geochronology of the Lac Shortt magmatic-hydrothermal system and REE-Au deposit clearly demonstrate that calc-alkaline magmatism was followed by syenitic magmatism, and subsequently by carbonatitic magmatism and carbo-hydrothermalism (Thorpe et al., 1984; Morasse, 1988; Prud'homme, 1990; See, 1994; Brisson, 1998). Geochemical (incompatible mobile and immobile trace element concentrations) and isotopic (Sr, C and O) analyses of in-situ magmatic and carbothermal calcite, dolomite, ankerite and siderite from the ores and associated alkaline primitive to evolved intrusions of the Lac Shortt gold-REE deposit, Abitibi, Canada indicate that the carbonatite was sourced from the Archean depleted mantle and exsolved a carbo-hydrothermal fluid enriched in REE and gold and that this fluid transported and deposited the gold and REE mineralization. Although $\delta^{13}C$ and $\delta^{18}O$ shows CO_3^{2-} anionic group gradually equilibrated with crustal components at lower temperature, $^{87}Sr/^{86}Sr_0$ data suggest that cations such as Sr^{2+}, Ca^{2+}, Mg^{2+}, Fe^{2+} and by inference Au^{+} and REE^{3+}, originated from the late-Archean, subcontinental depleted mantle.

Supplementary data to this article can be found online at http://dx.doi.org/10.1016/j.chemgeo.2014.08.021.

Acknowledgements

This study was made possible by NSERC and FRQNT grants to MJ and RS and by a FRQNT postdoctoral scholarship to ON. We would like to thank Professor Gema Olivo for kindly providing the samples. We would also like to thank Dr. A. Poirier and Dr. B. Galeb for help with the Sr isotope and laser ablation ICPMS analyses, Dr. JF. Hélie for help with the stable isotope analyses, Dr. P. Boulvais for discussions concerning the isotope results, L. Shi for help with the electron microprobe, R. Lapointe for help with numerous techniques, and M. Laithier and V. Horoi for help with the figures.

References

Andrade, F.R.D., Moeller, P., Lueders, V., Dulski, P., Gilg, H.A., 1999. Hydrothermal rare earth elements mineralization in the Barra do Itapirapua Carbonatite, southern Brazil; behaviour of selected trace elements and stable isotopes (C, O). Chem. Geol. 155, 91–113.

Ayer, J., Amelin, Y., Corfu, F., Kamo, S., Ketchum, J., Kwok, K., Trowell, N., 2002. Evolution of the southern Abitibi greenstone belt based on U-Pb geochronology; autochthonous volcanic construction followed by plutonism, regional deformation and sedimentation. Precambrian Res. 115, 63–95.
Bedard, L.P., 1988. Petrography and geochemistry of the Dolodau Stock; associated syenite and carbonatite, Canada(M.Sc Thesis) Université du Québec à Chicoutimi.
Bedard, L.P., Chown, E.H., 1992. The Dolodau dykes, Canada; an example of an Archean carbonatite. Mineral. Petrol. 46, 109–121.
Bell, K., 1989. Carbonatites, genesis and evolution. Ottawa-Carleton Geoscience Center, Proceeding of the 1986 GAC-MAC meeting, 618. Unwin Hyman Ltd., London.
Ben Othman, D., Arndt, N.T., White, W.M., Jochum, K.P., 1990. Geochemistry and age of Timiskaming alkali volcanics and the Otto syenite stock, Abitibi, Ontario. Can. J. Earth Sci. 27, 1304–1311.
Bigot, 2012. Les Minéralisations aurifères du gisement Archéen de Beatttie à Duparquet, Abitibi, Québec, Canada(MSc Thesis) Université du Québec à Montréal.
Bouabdellah, M., Hoernle, K., Kchit, A., Duggen, S., Hauff, F., Kluegel, A., Lowry, D., Beaudoin, G., 2010. Petrogenesis of the Eocene Tamazert continental carbonatites (central High Atlas, Morocco); implications for a common source for the Tamazert and Canary and Cape Verde Island carbonatites. J. Petrol. 51, 1655–1686.
Boulvais, P., Fourcade, S., Gruau, G., Moine, B., Cuney, M., 1998. Persistence of pre-metamorphic C and O isotopic signatures in marbles subject to Pan-African granulite-facies metamorphism and U–Th mineralization (Tranomaro, Southeast Madagascar). Chem. Geol. 150, 247–262.
Bourne, J.H., Bosse, J., 1991. Geochemistry of ultramafic and calc-alkaline lamprophyres from the Lac Shortt area, Quebec. Mineral. Petrol. 45, 85–103.
Brisson, H., 1998. Caractéristiques, chronologie et typologie des minéralisations aurifères de la région du Lac Shortt (Québec), sous-province archéenne de l'Abitibi(Ph.D. Thesis) Université du Québec à Chicoutimi.
Colvine, A.C., Springer, J.S., Troop, D.G., Andrews, A.J., Cherry, M.E., Durocher, M.E., Fyon, J. A., Lavigne Jr., M.J., Macdonald, A.J., Marmont, S., Poulsen, K.H., 1984. An integrated model for the origin of Archean lode gold deposits. Ontario Geological Survey OFR5524, Toronto, ON, Canada (194 pp.).
Corfu, F., 1993. The evolution of the Southern Abitibi Greenstone Belt in light of precise U-Pb geochronolgy. Econ. Geol. 88, 1323–1340.
Corfu, F., Krogh, T.E., Kwok, Y.Y., Jensen, L.S., 1989. U-Pb zircon geochronology in the southwestern Abitibi greenstone belt, Superior Province. Can. J. Earth Sci. 26, 1747–1763.
Eyal, M., Litvinovsky, B., Jahn, B.M., Zanvilevich, A., Katzir, Y., 2010. Origin and evolution of post-collisional magmatism; coeval Neoproterozoic calc-alkaline and alkaline suites of the Sinai Peninsula. Chem. Geol. 269, 153–179.
Fyon, J.A., Schwarcz, H.P., Crocket, J.H., 1984. Carbonatization and gold mineralization in the Timmins area, Abitibi greenstone belt; genetic links with Archean mantle CO_2; degassing and lower crustal granulitization. Program with Abstracts – Geological Association of Canada; Mineralogical Association of Canada: Joint Annual Meeting. 9, p. 65.
Groves, D.I., Goldfarb, R.J., Gebre-Mariam, M., Hagemann, S.G., Robert, F., 1998. Orogenic gold deposits: A proposed classification in the context of their crustal distribution and relationship to other gold deposit types. Ore Geol. Rev. 13, 7–27.
Jensen, E.P., Barton, M.D., 2000. Gold deposits related to alkaline magmatism. Rev. Econ. Geol. 13, 279–314.
Kerrich, R., Cassidy, K.F., 1994. Temporal relationships of lode gold mineralization to accretion, magmatism, metamorphism and deformation; Archean to present; a review. Ore Geol. Rev. 9, 263–310.
Kerrich, R., Fryer, B.J., King, R.W., Willmore, L.M., Van-Hees, E., 1987. Crustal outgassing and LILE enrichment in major lithosphere structures, Archean Abitibi greenstone belt; evidence on the source reservoir from strontium and carbon isotope tracers. Contrib. Mineral. Petrol. 97, 156–168.
Krystopowicz, N.J., Currie, C.A., 2013. Crustal eclogitization and lithosphere delamination in orogens. Earth Planet. Sci. Lett. 361, 195–207.
Martin, R.F., Sokolov, M., Magaji, S.S., 2012. Punctuated anorogenic magmatism. Lithos 152, 132–140.
Monecke, T., Kempe, U., Monecke, J., Sala, M., Wolf, D., 2002. Tetrad effect in rare earth element distribution patterns: a method of quantification with application to rock and mineral samples from granite-related rare metal deposits. Geochim. Cosmochim. Acta 66, 1185–1196.
Morasse, S., 1988. Geological setting and evolution of the Lac Shortt gold deposit, Waswanipi, Quebec, Canada, Department of Earth Sciences. Queen's University.
Mortensen, J.K., 1993. U-Pb geochronology of the eastern Abitibi Subprovince; Part 2, Noranda-Kirkland Lake area. Can. J. Earth Sci. 30, 29–41.
Mueller, W.U., Daigneault, R., Mortensen, J.K., Chown, E.H., 1996. Archean terrane docking; upper crust collision tectonics, Abitibi greenstone belt, Quebec, Canada. Tectonophysics 265, 127–150.
Nadeau, O., Stevenson, R., Jébrak, M., 2013. Depleted mantle as the source of gold in Archean alkaline magmatic-hydrothermal systems. Mineral. Mag. 76, p. 2152 (Abstract).
Parsons, G.E., 1948. Bidgood Kirkland Mine, Ontario. Canadian Institute of Mining and Metallurgy, Geological Division, Structural geology of Canadian ore deposits, pp. 653–658.
Pearce, N.J.G., Leng, M.J., Emeleus, C.H., Bedford, C.M., 1997. The origins of carbonatites and related rocks from the Gronnedal-Ika nepheline syenite complex, South Greenland; C-O-Sr isotope evidence. Mineral. Mag. 61, 515–529.
Prud'homme, N., 1990. Caracterisation petrographique et geochimique de la carbonatite et de la syenite de la mine Lac Shortt, Petrographic and geochemical characterization of the carbonatite and of the syenite of the Shortt Lake Mine, Canada(M.Sc Thesis) Université du Québec à Chicoutimi.
Pye, E.G., 1976. Geology of the Crow River area, District of Kenora (Patricia Portion). Ontario Geological Survey report no. 0826-9580Toronto, ON, Canada.
Richards, J.P., 2009. Postsubduction porphyry Cu-Au and epithermal Au deposits; products of remelting of subduction-modified lithosphere. Geology 37, 247–250.
Robert, F., 2001. Syenite-associated disseminated gold deposits in the Abitibi greenstone belt, Canada. Mineral. Deposita 36, 503–516.
Rock, N.M.S., 1986. The nature and origin of ultramafic lamprophyres; alnoeites and allied rocks. J. Petrol. 27, 155–196.
Rock, N.M.S., 1987. The nature and origin of lamprophyres; an overview. Geol. Soc. Spec. Publ. 30, 191–226.
Rock, N.M.S., 1988. Gold, porphyries and lamprophyres; a new genetic model. Abstr. Geol. Soc. Aust. 22, 307–312.
Rock, N.M.S., 1991. Lamprophyres. Blackie, Van Nostrand Reinhold, Glasgow, United Kingdom, New York, NY, United States, United Kingdom (285 pp.).
Rock, N.M.S., Groves, D.I., 1988a. Can lamprophyres resolve the genetic controversy over mesothermal gold deposits? Geology 16, 538–541.
Rock, N.M.S., Groves, D.I., 1988b. Do lamprophyres carry gold as well as diamonds? Nature 332, 253–255.
Rock, N.M.S., Duller, P., Haszeldine, R.S., Groves, D.I., 1987. Lamprophyres as potential gold exploration targets; some preliminary observations and speculations. 11. Publication – Geology Department and Extension Service, University of Western Australia, pp. 271–286.
Rock, N.M.S., Groves, D.I., Ramsay, R.R., 1988. Lamprophyres; a girl's best friend? Publication – Geology Department and Extension Service, University of Western Australia. 12, pp. 295–308.
Rock, N.M.S., Groves, D.I., Perring, C.S., Golding, S.D., 1989. Gold, lamprophyres, and porphyries; what does their association mean? Econ. Geol. Monogr. 6, 609–625.
Rowins, S.M., Cameron, E.M., Lalonde, A.E., Ernst, R.E., 1993. Petrogenesis of the late Archean syenitic Murdock Creek Pluton, Kirkland Lake, Ontario; evidence for an extensional tectonic setting. Can. Mineral. 31, 219–244.
Saunders, A.D., Tarney, J., 1984. Geochemical characteristics and tectonic significance of back-arc basins. Geol. Soc. Spec. Publ. 16, 59–76.
See, J., 1994. L'analyse des inclusions fluides et magmatiques des dépôts aurifères dans la région du Lac Shortt, Abitibi, Québec: l'interprétation thermodynamique et métaliogénétique du rôle des fluides minéralisants à i'Archéen(Ph.D. Thesis) Université du Québec à Chicoutimi, (240 pp.).
Smith, P.M., 1986. Duport, a structurally controlled gold deposit in northwestern Ontario, Canada. GOLD '86, Toronto, ON, Canada, Canada, pp. 197–212.
Smithies, R.H., Champion, D.C., 1999. Late Archaean felsic alkaline igneous rocks in the Eastern Goldfields, Yilgarn Craton, Western Australia; a result of lower crustal delamination? J. Geol. Soc. Lond. 156, 561–576 (Part 3).
Sun, S.S., 1980. Lead isotopic study of young volcanic rocks from mid-ocean ridges, ocean islands and island arcs. Philos. Trans. R. Soc. A Math. Phys. Sci. 297, 409–445.
Thomson, J.E., 1950. Geology of the main ore zone at Kirkland Lake; introduction and general description. USGS Economic Geology of Ore deposits. 57, Part 5, pp. 55–103.
Thorpe, R.I., Guha, J., Franklin, J.M., Loveridge, W.D., 1984. Use of a Superior Province lead isotope framework in interpreting mineralization stages in the Chibougamau District. Spec. Vol. Can. Inst. Min. Metall. 34, 496–516.
Tilton, G.R., Bell, K., 1994. Sr-Nd-Pb isotope relationships in Late Archean carbonatites and alkaline complexes: Applications to the geochemical evolution of Archean mantle. Geochim. Cosmochim. Acta 58, 3145–3154.
Veizer, J., Hoefs, J., Lowe, D.R., Thurston, P.C., 1989a. Geochemistry of Precambrian carbonates; II, Archean greenstone belts and Archean sea water. Geochim. Cosmochim. Acta 53, 859–871.
Veizer, J., Hoefs, J., Ridler, R.H., Jensen, L.S., Lowe, D.R., 1989b. Geochemistry of Precambrian carbonates; I, Archean hydrothermal systems. Geochim. Cosmochim. Acta 53, 845–857.
Veksler, I.V., 2005. Element enrichment and fractionation by magmatic aqueous fluids; experimental constraints on melt-fluid immiscibility and element partitioning. Short Course Notes Geol. Assoc. Can. 17, 69–85.
Wilhelmy, J.F., Kieller, B., 1986. Évaluation du potentiel économique d'une carbonatite. Centre de recherche minérales, Corporation Faconbridge Copper, document no. 86-MI-024.
Williams-Jones, A.E., Migdisov, A.A., Samson, I.M., 2012. Hydrothermal mobilisation of the rare earth elements; a tale of 'ceria' and 'yttria'. Elements 8, 355–360.
Wilson, M., 1989. Igneous petrogenesis. Springer, Unwin Hyman, London – Boston (466 pp.).
Wyman, D.A., Kerrich, R., 1987. Archean lamprophyres; I, Distribution and tectonic setting. Program with Abstracts – Geological Association of Canada; Mineralogical Association of Canada: Joint Annual Meeting. 12, p. 102.
Wyman, D., Kerrich, R., 1988. Alkaline magmatism, major structures, and gold deposits; implications for greenstone belt gold metallogeny. Econ. Geol. Bull. Soc. Econ. Geol. 83, 454–461.
Wyman, D., Kerrich, R., 1989. Archean shoshonitic lamprophyres associated with Superior Province gold deposits, distribution, tectonic setting, noble metal abundances, and significance for gold mineralization. Econ. Geol. Monogr. 6, 651–667.